Simulations of Electromagnetic Turbulence and Transport in Tokamak Plasmas

P. B. Snyder, G. W. Hammett, M. A. Beer, W. Dorland[1]

Plasma Physics Laboratory, Princeton University, Princeton NJ 08543 USA.
[1] University of Maryland, College Park, MD, USA

An electromagnetic gyrofluid model is developed to study turbulent processes in toroidal plasmas. The model is benchmarked against kinetic theory, and used to study turbulence arising from both the finite-β Ion Temperature Gradient (ITG) mode and kinetic shear Alfvén instabilities. The inclusion of electromagnetic effects is found to lead to a significant quantitative reduction in turbulent heat transport at modest β values. A dramatic increase in heat transport occurs as the Ideal-MHD ballooning β limit is approached, associated with a qualitative change in the dominant scales of the turbulence. In addition, Alfvénic turbulence is found to be important at characteristic edge parameters, and may explain the increased heat conductivity observed near the plasma edge.

I. Introduction

Gyrokinetic particle and gyrofluid simulations of tokamak core plasmas have generally invoked the electrostatic approximation and used adiabatic passing electrons. In addition to the usual gyrokinetic ordering, such simulations also assume the following separation of time scales, $\omega \sim k_\parallel v_{ti} \sim \omega_* \sim \omega_D \ll k_\parallel v_A, k_\parallel v_{te}, \omega_{ETG}$. Here ω is a typical frequency, $k_\parallel$ and $k_\perp$ are typical wavenumbers parallel and perpendicular to the magnetic field, ρ is the gyroradius, $v_{ti} = \sqrt{T_i/m_i}$ is the ion thermal speed, v_A is the Alfvén speed, ω_D is the curvature and ∇B drift rate, ω_* is the usual ion diamagnetic frequency, while ω_{ETG} is a frequency characteristic of electron drift modes, which typically have $k_\perp \rho_e \sim 1$. The above ordering, particularly $\omega_* \ll k_\parallel v_A$, breaks down in the moderate to high β regimes characteristic of many fusion experiments and fusion reactor designs.

With moderate plasma β, there are significant finite-β modifications to drift modes such as the Ion Temperature Gradient (ITG) mode as well as nonlinear coupling to Alfvén waves. The Alfvén waves themselves can also be unstable and drive turbulent transport. In particular, when the ion temperature gradient is finite, ion drift resonance drives the Alfvén wave unstable below the Ideal MHD ballooning β limit.

To incorporate finite-β effects and Alfvén waves, we modify the above ordering as follows:

$$k_\perp^{-1} \sim \rho_i \gg \rho_e, c/\omega_{pe} \qquad \omega \sim k_\parallel v_{ti} \sim \omega_* \sim \omega_D \sim k_\parallel v_A \ll k_\parallel v_{te}, \omega_{ETG}. \qquad (1)$$

Note that the scales on the left hand side are independent of the electron mass, while the lengths on the right are proportional to $m_e^{1/2}$, and the frequencies on the right scale with $m_e^{-1/2}$. The above ordering can hence be implemented via an expansion in the mass ratio m_e/m_i while taking β to be order one.

II. The Model

The ions are modeled with a set of six moments of the electromagnetic gyrokinetic equation[1, 2]. The moment hierarchy is truncated using closures analogous to those derived
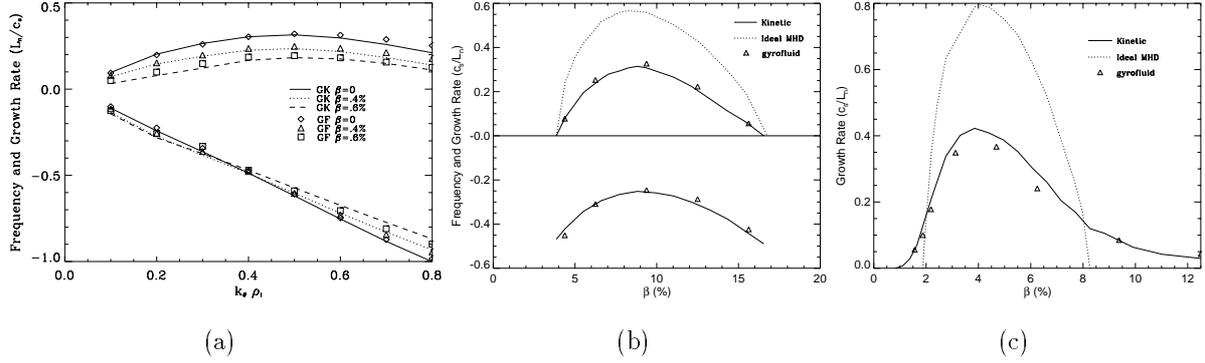
(a)   (b)   (c)

Figure 1: Benchmarks with linear kinetic codes. Fig. (a) plots the linear growth rate (positive) and frequency (negative) spectra of the ITG mode for $\beta = 0$, $\beta = .4\%$, and $\beta = .6\%$, with $\eta_i = \eta_e = 5$, $R/L_n = 3$, $s = 1$, $q = 2$ and $\tau = T_{i0}/T_{e0} = 1$. The gyrofluid result is compared with results from M. Kotschenreuther's `GS2`[6] linear gyrokinetic code. Fig. (b) plots the frequency (negative) and linear growth rate (positive) of the toroidal Alfvén mode vs. β, with a flat temperature profile ($\eta_i = \eta_e = 0$), $k_\theta \rho_i = 0.5$, $\epsilon_n = 0.25$, $s = 1$, $q = 2$, and $\tau = 1$. An $s - \alpha$ equilibrium model is used, and for these parameters, $\alpha = 16\,\beta$. The gyrofluid model is compared to kinetic theory [7]. The MHD prediction is shown for comparison. In (c) a finite ion temperature gradient ($\eta_i = 2$) is added, and the gyrofluid model is again compared to growth rates predicted by Hong et al.[7]. With finite η_i, the Alfvén wave becomes unstable both below the Ideal-MHD β-limit and into the "second stability" region. The gyrofluid model is able to reproduce both of these effects.

by [3–5]. The resulting equations are similar to the electrostatic toroidal gyrofluid equations of Beer[5], with the addition of magnetic induction, linear and nonlinear magnetic flutter, and magnetic finite-Larmor-radius terms.

The electron equations are also derived from the electromagnetic gyrokinetic equation[1], with the ordering in Eq. 1 carefully followed for both ion and electron fluctuations. To lowest order in m_e/m_i a natural truncation of the moment hierarchy occurs, and the normalized electron equations become:

$$\frac{\partial n_e}{\partial t} + \mathbf{v}_E \cdot \nabla n_e + B\tilde{\nabla}_\parallel \frac{u_{\parallel e}}{B} - i\omega_* \phi + 2i\omega_d \big(\phi - \frac{n_e}{\tau} - T_e\big) = 0, \tag{2}$$

$$\frac{\partial A_\parallel}{\partial t} + \tilde{\nabla}_\parallel \phi - \frac{1}{\tau}\tilde{\nabla}_\parallel n_e - \frac{1}{\tau}i\omega_* A_\parallel = \sqrt{\frac{\pi}{2\tau}\frac{m_e}{m_i}} |k_\parallel| u_{\parallel e} + \nu_{ei}\frac{m_e}{m_i}(u_{\parallel e} - u_{\parallel i}), \tag{3}$$

where the T_e term in Eq. 2 will be calculated by numerically inverting the equation $\tilde{\nabla}_\parallel T_e = -\eta_e i\omega_* A_\parallel/\tau$, which expresses the constraint in this ordering that the total electron temperature is constant along perturbed magnetic field lines. The models of electron Landau damping and electron-ion collisions which appear on the right of Eq. 3 are formally ordered $\mathcal{O}(\sqrt{m_e/m_i})$. These terms provide dissipation and their impact will be studied in nonlinear simulations.

The above set of electron equation represents a fairly simple and elegant model of the electron dynamics on Alfvén and ion scales. While only two moment equations need be solved, the physics content of a full six moment model has been incorporated to lowest order in m_e/m_i.
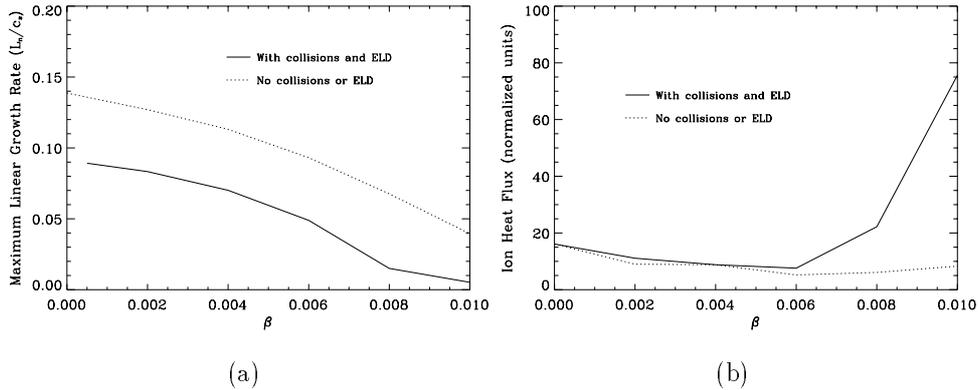
(a)   (b)

Figure 2: Maximum linear growth rate (a) and ion heat flux (b) vs. β. All runs in $s - \alpha$ geometry with $s = 1$, $q = 2$, $L_n/R = 1/3$, $\eta_i = \eta_e = 3$. Results both with and without electron Landau damping and electron-ion collisions are shown.

Though the model is simple, it represents a very substantial improvement over the adiabatic electron models $(n_e/\tau = \phi - \langle\phi\rangle_{surface})$ that have been used to describe the passing electrons in most previous gyrofluid and gyrokinetic particle simulations. In addition to finite-β effects and Alfvén wave dynamics, the above model also incorporates electron $\mathbf{E} \times \mathbf{B}$, curvature, and ∇B drift motion, as well as the $\mathbf{E} \times \mathbf{B}$ nonlinearity and four additional nonlinear terms due to magnetic flutter. The equation system is completed with the gyrokinetic Poisson's Equation and Ampere's Law[1].

The model accurately describes finite-β effects on the ITG mode, as well as capturing the physics of kinetic shear Alfvén instabilities, including the ion drift resonance effect, as demonstrated by the benchmarks in Fig. 1. Furthermore, the model successfully removes the short electron space and time scales, and allows practical three-dimensional nonlinear simulation.

III. Nonlinear Results

Nonlinear simulations are carried out in a toroidal flux tube geometry using an updated version of the `Gryffin` gyrofluid code.

Fig. 2 shows the results of a scan vs. β, holding other equilibrium parameters fixed. At low β, both linear growth rates and the nonlinear flux decreases with β. However, as the Ideal ballooning limit $(\beta_c = 1.1\%)$ is approached, the nonlinear flux increases even though the linear growth rate continues to decrease. In the presence of electron dissipation, dominantly electron Landau damping, the increase in flux near β_c is quite substantial. The increased flux is believed to be due to the kinetic ion drift resonance instability of the Alfvén wave near β_c. Note that while the ITG is the dominant instability in Fig. 2a and its growth rate decreases with β, the subdominant kinetic Alfvén wave exists also, and it becomes unstable with a growth rate increasing with β as β_c is approached. It appears that despite its small linear growth rate, the Alfvén instability may nonlinearly saturate at high amplitude near β_c and dominate the turbulent steady state. Fig. 3 illustrates the dramatic change in characteristic turbulent length and time scales that occurs as β approaches β_c.
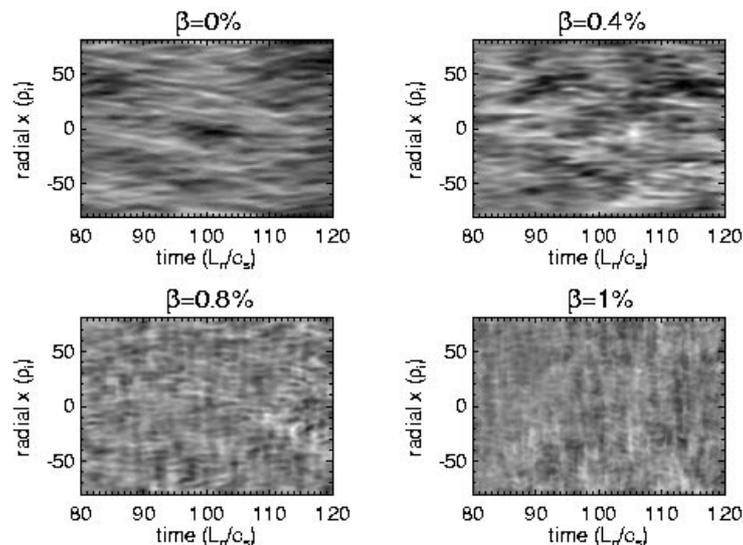
Figure 3: Contour plots of the electrostatic potential vs. time and radius, at four values of the plasma β chosen from Fig. 2. The plots reveal a shift toward long wavelengths and short time scales as the MHD $\beta_c = 1.1\%$ is approached.

One important limitation of earlier electrostatic simulations has been their inability to predict the dramatic increase in heat conductivity often seen near the edge of tokamak experiments. The figure at right compares nonlinear electromagnetic and electrostatic simulation results to measured ion heat conductivity near the edge of a TFTR L-mode shot. Quantitative agreement is not expected, due to the absence of important effects such as trapped electrons and impurities from the simulations. However, the electromagnetic simulations appear to capture physics important for understanding edge transport. The increase in transport with radius is due to the same effect as in Fig. 2b. The ballooning limit is approached in the edge despite low β, because of high q and sharp density gradients.
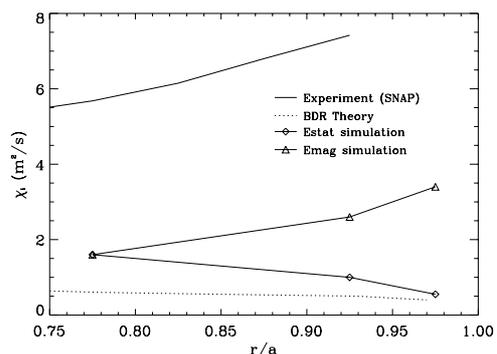
[1] BRIZARD, A., Phys. Fluids B **4** (1992) 1213.

[2] HAHM, T. S., LEE, W. W., and BRIZARD, A., Phys. Fluids **31** (1988) 1940.

[3] HAMMETT, G. and PERKINS, F., Phys. Rev. Lett. **64** (1990) 3019.

[4] DORLAND, W., *Gyrofluid Models of Plasma Turbulence*, PhD thesis, Princeton University, 1993.

[5] BEER, M. A., *Gyrofluid Models of Turbulent Transport in Tokamaks*, PhD thesis, Princeton University, 1995.

[6] KOTSCHENREUTHER, M., REWOLDT, G., and TANG, W. M., Computer Physics Communications **88** (1995) 128.

[7] HONG, B.-G., HORTON, W., and CHOI, D.-I., Phys. Fluids B **1** (1989) 1589.